

Aeroacoustic performances of a low-noise airfoil cascade with serrated leading edges: predictions and measurements

Cyril Polacsek, Martin Buszyk, Raphaël Barrier, Vincent Clair, Edouard Salze

▶ **To cite this version:**

Cyril Polacsek, Martin Buszyk, Raphaël Barrier, Vincent Clair, Edouard Salze. Aeroacoustic performances of a low-noise airfoil cascade with serrated leading edges: predictions and measurements. ICAS 2022, Sep 2022, STOCKHOLM, Sweden. hal-03938107

HAL Id: hal-03938107
https://hal.science/hal-03938107

Submitted on 13 Jan 2023

HAL is a multi-disciplinary open access archive for the deposit and dissemination of scientific research documents, whether they are published or not. The documents may come from teaching and research institutions in France or abroad, or from public or private research centers.

L'archive ouverte pluridisciplinaire **HAL**, est destinée au dépôt et à la diffusion de documents scientifiques de niveau recherche, publiés ou non, émanant des établissements d'enseignement et de recherche français ou étrangers, des laboratoires publics ou privés.

AEROACOUSTIC PERFORMANCES OF A LOW-NOISE AIRFOIL CASCADE WITH SERRATED LEADING EDGES: PREDICTIONS AND MEASUREMENTS

C. Polacsek[1], M. Buszyk[1], R. Barrier[2], V. Clair[3] & E. Salze[3]

[1]ONERA, DAAA, Numerical Aeroacoustic Unit, F-92322 Châtillon, France
[2]ONERA, DAAA, Helicopter, Propeller & Turbomachinery Unit, F-92190 Meudon, France
[3] LMFA, Ecole Centrale de Lyon, 69134 - Ecully, France

Abstract

This paper discusses the performances of a low-noise airfoil cascade with leading edge serrations designed by ONERA and recently tested in a laboratory facility at Ecole Centrale de Lyon. Available predictions on flow and radiated sound field assessed on the reference and treated cases using analytical and numerical methods are compared to the first post-processed measurements. A fairly good agreement is obtained on turbulent grid flow characteristics, pressure vane coefficient, and radiated sound fields downstream the cascade. In particular, the expected noise reductions of 4-5 dB pointed out from pre-test works are confirmed by the experiments, delivering sound power attenuation spectra (up to 6 dB) for the two selected designs closely captured by the Lattice Boltzmann solutions (detailed in a complementary paper) at the computed regime.

Keywords: Turbofan noise ; cascade test rig ; noise reduction concepts ; serrations

1. Introduction

The interaction between the turbulent fan wakes and the outlet guide vanes (OGV) is known to be a major source contributor to the broadband noise emission from turbofan engines, particularly at the approach (APP) operating point condition. Reducing the turbulence-airfoil source mechanism to lower the overall sound levels is one of the priorities for engine manufacturers. In this scope, different reduction technologies have been designed and are being tested numerically and experimentally in the framework of the H2020 European project InnoSTAT (Innovative stators, https://cordis.europa.eu/project/id/865007), started in 2020. Several of the concepts proposed rely on passive treatments aiming to reduce the interaction noise sources located in the leading edge (LE) region of the airfoil. With this aim, leading edge serrations, initially proposed by ONERA [1] during the European project FLOCON, have been extensively studied [1-5] and are believed to be one of the most relevant passive treatment able to provide a significant noise reduction with acceptable aerodynamic penalties [5].

The first part of the project is devoted to a simplified configuration consisting in a 7-vane rectilinear cascade impacted by an isotropic turbulence generated from a turbulence grid and tested in the anechoic wind tunnel of Ecole Centrale de Lyon (ECL) [6]. ONERA is contributing to this project through two main activities: (i) the design of low-noise OGV prototypes based on LE serrations and (ii) the assessment of acoustic performances using analytical and numerical methods. A part of this work has been already presented and recently published by Buszyk et al. [7], focusing on numerical simulations based on linearized Euler calculations performed with an in-house CAA solver and synthetic turbulence model adapted to the present cascade configuration. Only a short overview of the prediction methods and key results are reported again in this paper, mainly dedicated to the first comparisons between the available predictions and the measurements,

freshly post-processed from the ECL tests achieved by May 2022. Complementary predictions on the KCA cascade using the LBM approach are discussed in another communication [8], through a collaborative work between ONERA and Cerfacs.
The paper is structured as follows. The experimental set-up is presented in Section 2 and the low-noise serrated vanes designed by ONERA in Section 3. Section 4 gives a short overview of prediction methods with a summary of aerodynamic and acoustic assessments. Then, detailed comparisons with the measurements are discussed in Section 5 and conclusions with key results are addressed in Section 6.

2. Experimental set-up

2.1 ECL KCA rig with turbulence grid and rectilinear cascade

The experiments are conduced in the main subsonic anechoic wind tunnel (KCA rig) at École Centrale de Lyon, France. The flow is generated by a 800 kW Howden double stage centrifugal fan, delivering a mass flow rate around 20 kg/s. Air passes through a settling chamber including honeycombs and several wiremeshes designed to reduce free stream turbulence. Acoustic liners on the wind tunnel walls and baffled silencers allow to reduce the noise level and to prevent contamination of acoustic measurements performed in the anechoic chamber. This results in an air flow with a low background noise and low residual turbulence less than 0.5%. A dedicated test section, presented in Fig. 1, has been designed for this experimental campaign. A 0.5 m long contraction adapts the test section from 0.56 *0.56 m! to 0.56 *0.2 m!. Several vein pieces with suited bends are connected from the wind tunnel convergent up to the cascade front (see Fig. 1c) in order to ensure an homogeneous mean flow with the desired flow angle of attack (AoA). A turbulence grid (sketched in Fig. 1d), made of rectangular rods (D = 1 cm, L = 4 cm), can be inserted just upstream of the contraction, as visible in Fig. 1a. The leading edge of the central vane is located at about 0.5 m downstream of the contraction. The vertical side plates are guiding the flow down to the trailing edge of the cascade, while the horizontal plates extend downstream of the cascade as a semicircle centered on the trailing edge of the central vane, with a radius of 0.45 m. The 7-vane cascade is equipped with 7310 NACA airfoils, c = 120 mm in chord and L_v = 200 mm in span. The inter-vane space is equal to 85 mm.

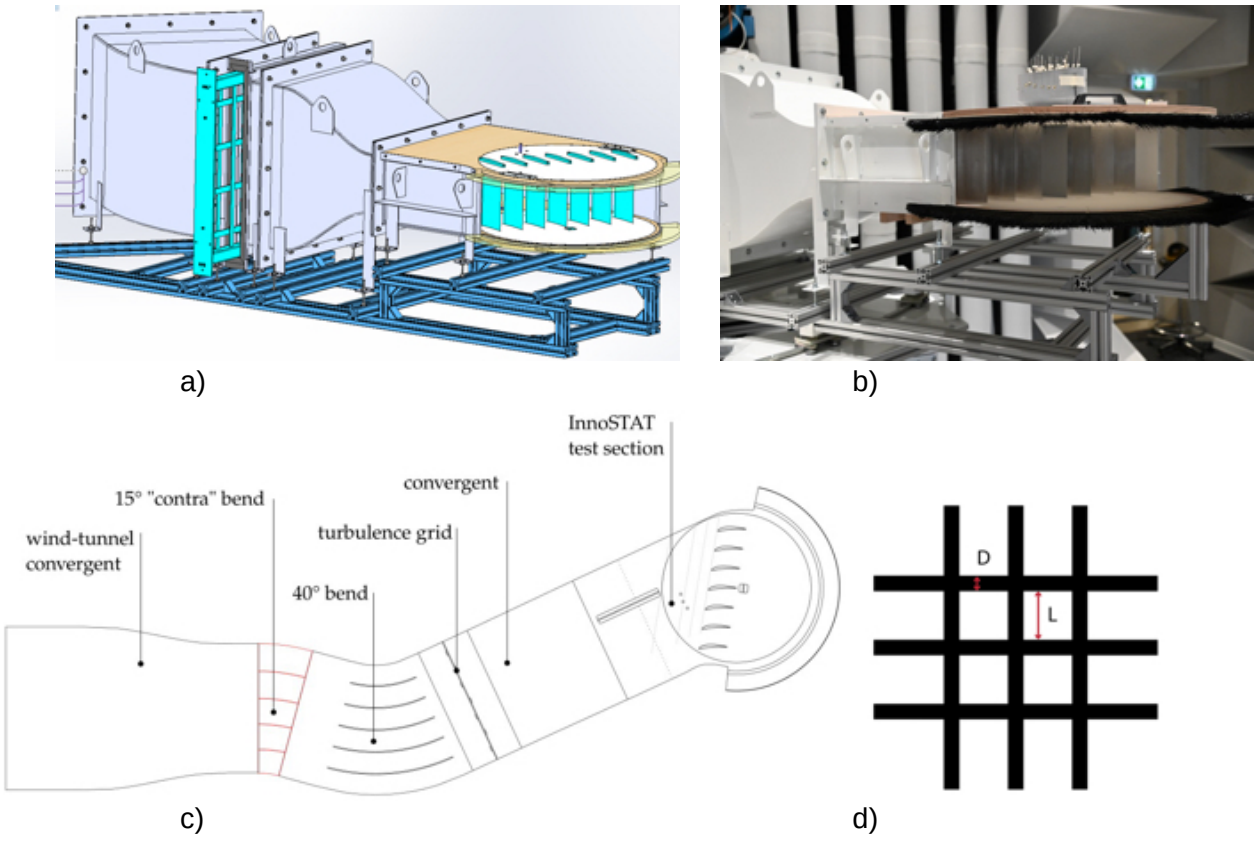


Figure 1 – (a) Schematic view of test facility, (b) side picture, (c) rig cut view, (d) turbulence grid.

Soft brushes are placed at the edges of the cascade plates (see Fig. 1b) to minimize the tip vortices in the boundary layer that could create spurious noise [6]. The vanes are mounted on disks embedded in the horizontal plates, which allows for the rotation of the cascade around the trailing edge of the central vanes to adjust the angle β_c between the incident flow and the normal to the cascade frontline (see Fig. 2). The stagger angle is kept at a constant value $\chi = 13°$, the β_c angle has a nominal value $\beta_c = 34°$ and can vary in the range $\beta_c = 34° \pm \Delta\beta_c$.

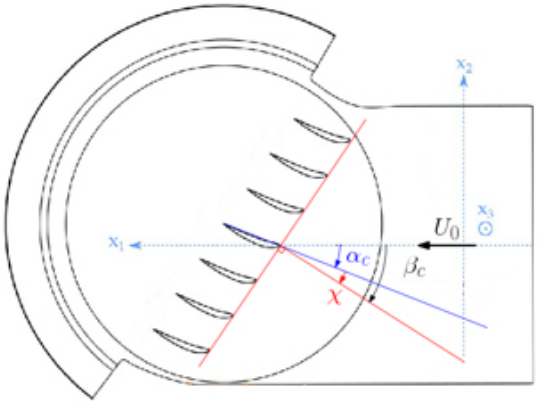


Fig. 2 – Definition of the stagger angle χ, the incidence angle α_c and $\beta_c = \alpha_c + \chi$.

2.2 Test matrix with main instrumentation

The present study only concerns the reference cascade and the two low-noise cascades with Onera designs, denoted ON1 and ON2. The test matrix with main instrumentation discussed in this paper is summarized in Table 1. Six flow speeds (U_0 increased from 45 to 182 m/s), plus a no-flow case, have been captured. The nominal AoA is set to 34°, and incidence effect is measured for specific deviations ±" β_c. Basic aerodynamic measurements are achieved by means of inflow hot-wire probes (mainly used to assess the turbulent grid flow characteristics) and by using static pressure probes (aiming to assess the vane forces and wall pressure coefficients). To prevent from vibration issues, the hot-wire measurements are acquired at a maximum speed of 100 m/s. Acoustic field is priory measured by means of a farfield microphone antenna (see Section 2.3), but some in-duct measurements using flush-mounted microphones (lines upstream the leading edge and behind the trailing edge of the middle vane) are also available. The data discussed in this paper are colored in red and in red bold for the flow speed at 117 m/s, corresponding to the flow condition of the numerical simulations. Approximative operating point conditions for approach (APP) and cutback (CUTB) are also indicated.

Table 1 – Main test matrix

Flow speed, U_0 (m/s)	β_c (deg)	Hot wire at mid-span (U_0 < 100 m/s and β_c =34°)	Wall pressure probes (middle vane)	Microphones	Ref.	Design ON1	Design ON2
45, 85,100,150 **117 (∼APP)** 182 (∼CUTB)	34°± " β_c	Velocity profiles Turbulence grid flow characteristics	Wall pressure coef. (mid-span)	Upstream line (duct casing) Circular antenna (farfield)	✓	✓	✓

2.3 Flow characterization and acoustic measurements

The locations of the aerodynamic measurements are displayed in Fig. 3. A set of static pressure probes is flush-mounted in the transverse direction in the lower wall of the test section, downstream of the contraction. The static pressure probes are used to verify that the flow is homogeneous upstream of the cascade despite the presence of the bend. A series of hot-wire velocity measurements are realized at different locations in the test section. Measurements in the boundary layer of the duct are performed just downstream of the contraction (see Fig. 3, top right). Velocity

profiles are measured in the mid-span plane over lines parallel to the cascade front line located 0.2 m and 0.05 m upstream of the cascade with both a single wire probe and an X wire probe (see Fig. 3, bottom right) to have access to two velocity components. Velocity profiles are also measured in the mid-span plane over a line parallel to the cascade trailing edge line located 0.015 m downstream of the trailing edges.
The upstream hot-wire measurements are performed only for the reference geometry at the nominal value of β_c. Finally, airfoil chordwise probes are distributed at mid-span, over the pressure and suction sides of the reference middle vane (see Fig. 4), in order to measure the wall pressure coefficients.
Acoustic measurements are performed both upstream and downstream of the cascade. The positions of the totalizing 43 microphones are shown in Fig. 5. A linear array comprising 26 microphones is located upstream of the cascade. This array can be used to separate the acoustic waves propagating in the upstream and downstream directions and thus isolate the upstream radiation from the cascade. Three microphones are located just downstream of the trailing edge of the central blade. A farfield circular array containing 14 microphones is centered on the trailing edge of the central vane with a radius of 1.95 m. The microphones are positioned in the mid-span plane, with an angular spacing of 10° from $-90°$ to $+90$ °. No microphones are located in the wake of the cascade between $-20°$ and $+40°$ where a non-negligible flow is present.

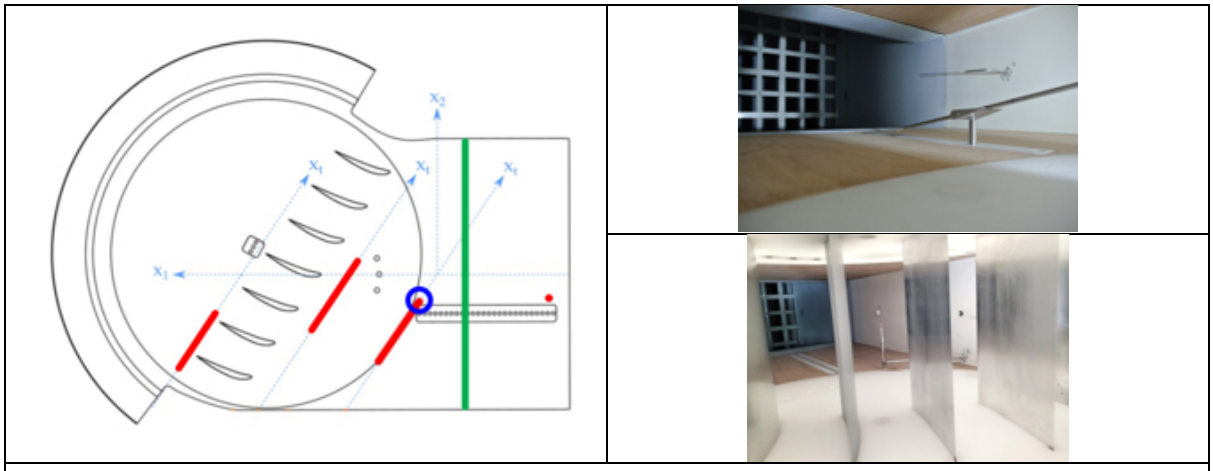


Fig. 3 — (left) positions of the static pressure probes in green and of the hot-wire measurements in red. (right, top) Picture of the hot-wire probes used for the boundary layer measurements. (right, bottom) Picture of the X wire probe used for the 2 components velocity measurements.

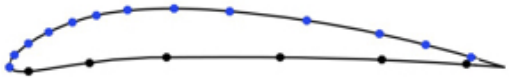


Figure 4 – Static pressure probes around the airfoil.

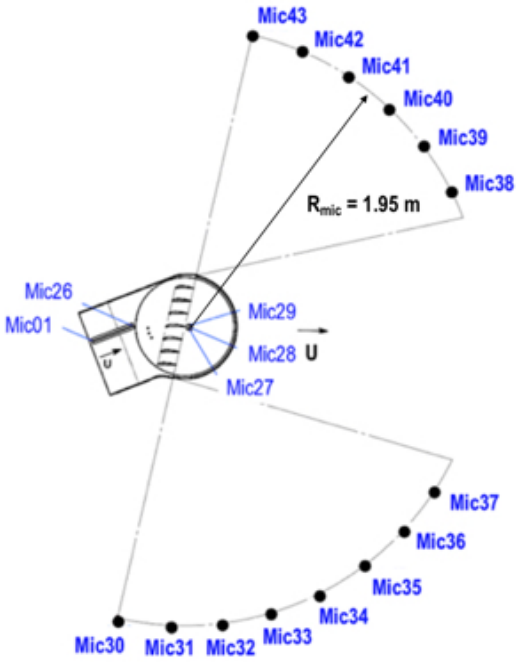


Figure 5 – Induct mics. and farfield antenna.

3. Low-noise serrated vanes

As already discussed by Buszyk et al. [7], the leading edge serrations based on regular sinusoidal patterns were designed by applying empirical rules and backgrounds and following the recent work published by Polacsek et al. [5]. The serration wavelength λ_s was set equal to twice the expected TLS (integral length scale) from the turbulence grid (TLS = 8 mm), and the ratio h_s / λ_s (h_s, the serration amplitude) was set equal to 1, keeping the mean chord equal to the reference chord ($c_{mean} = c_{ref}$). This 2D flat plate design was extended to the actual 3D airfoil by applying a suited morphing of the squeleton (with respect to thickness and camber laws) using an in-house modeler developed by Barrier. A first design (design 1) so obtained is shown in Fig. 6, left. A second design aiming to reduce the aerodynamic penalties has been proposed by imposing the reference chord at the roots (Fig. 6, right), instead at sinus cancellation. As shown in Sections 4-5, this simple increase of the mean chord ($c_{mean} = c_{ref} + h_s$) has led to a significant decrease of the pressure loss and outlet angle deviation, with almost no impact on acoustic performances. These two treatments were approved by the InnoSTAT Consortium and the CAD geometries were provided to COMOTI (InnoSTAT partner) in charge of the manufacturing. A photography of a manufactured vane (design 1) including sided-attachments for practical implementation in the rig is shown in Fig. 7.

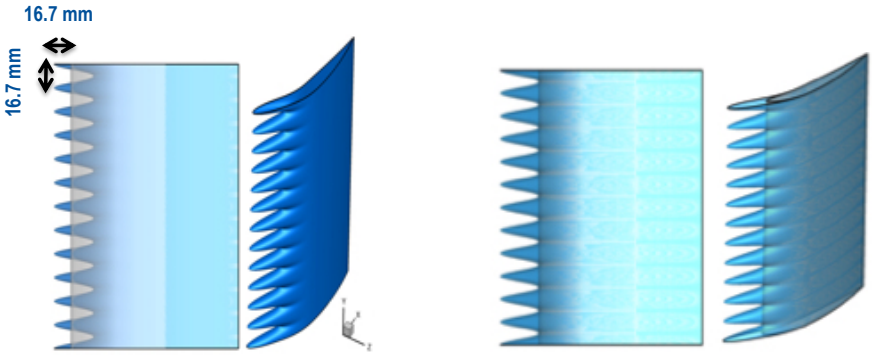


Figure 6 – 2D and 3D plots of ONERA's selected geometries: design ON1 (left) and ON2 (right).

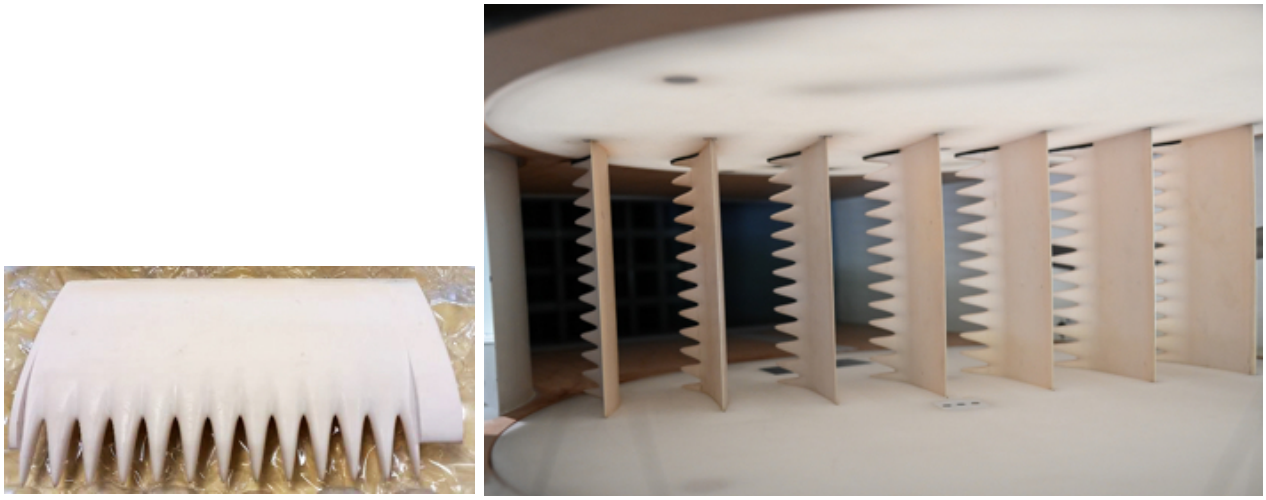


Figure 7 – Photos of manufactured serrated vane (design ON1) with sided attachments (left) and mounted on the 7-vanes cascade of the test rig (rear view, right).

4. Aerodynamic control and noise reduction predictions

4.1 Brief overview of prediction methods

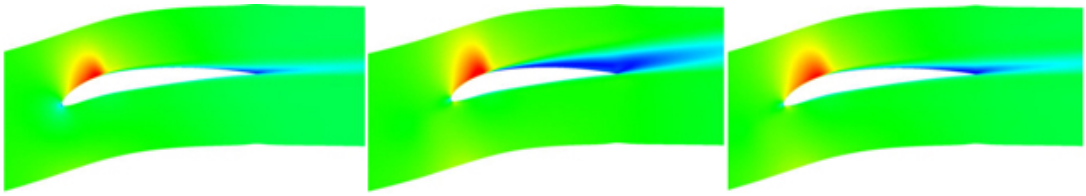
Several ways have been considered in this project to try to assess the acoustic performances of the low-noise airfoil cascade, relying on empirical, analytical and numerical approaches. The empirical "log law" evidenced by Paruchuri et al. [3] has been adopted to get a rough evaluation of the sound power level reduction, " PWL (DeltaPWL), as a function of a specific Strouhal number, St:

$$\text{" PWL(dB)} = 10\log(St) + 10, \text{ with } St = fh_s/U_0 \quad (1)$$

The Wiener-Hopf (WH) formulation developed by Ayton [9] and slightly adapted by Buszyk for finite span airfoil applications (see Appendix in Ref. [5]), has been used to predict the DeltaPWL at certification operating points (OP) [7]. Then, two complementary numerical methods have been proposed for more reliable predictions. (i) using an in-house CAA code (*sAbrinA*) solving the linearized Euler equations coupled with a synthetic turbulence model presented in detail in [7], and (ii) using the Lattice Boltzmann method (LBM) and the dedicated code *ProLB* with first simulations discussed in [8]. The FWH (Ffowcs Williams and Hawkings) analogy is used with the CAA (and when assessing non-direct LBM solution) to predict the radiated sound field relying on the turbulent pressure over the vane wall. More recent LBM simulations are also discussed in a second ICAS paper [10], through a collaborative work with Cerfacs. Besides these methods mostly devoted to acoustics, RANS calculations performed by ONERA (using *elsA* code) have been conducted to check the aerodynamic performances of the serrated airfoil cascade [7] and to compare with the LBM mean flow solutions [8,10]. Only the results issued from these different prediction tools (please refer to aforesaid works for more details) are brought back in the present paper.

4.2 Aerodynamic penalties

As mentioned above, RANS calculations have been performed to check the aerodynamic behavior of the treated geometries by comparison to the reference one, by focusing on the approximative APP condition (Mach = 0.34) and at the aerodynamic design point (ADP) roughly associated to Mach 0.67. Although the aerodynamic penalties are found to be rather weak at APP, aerodynamic performances are significantly deteriorated at ADP for the initial treatment (design 1). For this reason, a second design (plotted in Fig. 4, right) simply consisting in an increase of the mean chord ($c_{mean} = c_{ref} + h_s$) has been successfully drawn. Comparisons between these two designs and the baseline case are visualized in Fig. 8, in terms of Mach number contour maps at ADP, and summarized in Table 2, in terms of aerodynamic penalties at APP and ADP. The deviations for total pressure loss coefficient and outlet angle (remaining swirl) are respectively reduced to -0.1 point and to +0.8 deg. at ADP with the second design.



(a) baseline (b) design 1 (c) design 2

Figure 8 – Mach number (levels between 0.1 and 1.2) contour maps at ADP.

Table 2 – Summary of predicted aerodynamic performances

	baseline (reference)	design 1	design 2
Total pressure loss coefficient at APP	0.9970	0.9956 (-0.14 pt.)	0.9960 (-0.10 pt.)
Total pressure loss coefficient at ADP	0.9880	0.9720 (-1.60 pt.)	0.9820 (-0.60 pt.)
Outlet angle (remaining swirl) at APP	2.1°	3.9° (+ 1.8°)	2.6° (+ 0.5°)
Outlet angle (remaining swirl) at ADP	2.5°	6.3° (+ 3.8°)	3.3° (+ 0.8°)

4.3 Acoustic performances

Acoustic predictions based on analytical model are very fast and can be applied for several flow speed conditions (without incidence effects, assuming the incoming flow is fully aligned to the chord of the flat plate). On the other hand, numerical simulations based on CAA and LBM being much more time consuming have been focused on the APP condition with the nominal AoA (equal to 34 deg.). The CAA was conducted with slightly different values for Mach and AoA (pre-test conditions given earlier in the project), but these small deviations are believed to have negligible impact on the radiated sound field [7]. The acoustic performances obtained on the low-noise designs with prediction tools proposed by ONERA are summarized here, whereas more sound field analyzes are discussed in Section 5 when comparing to the experimental results. The spectra of sound power attenuation (Delta PWL) obtained from the WH calculations at the 3 certification OP are plotted in Fig. 9, left. Another solution at Mach = 0.3 (APP condition used for CAA) is also indicated, showing very small deviations compared to the solution at Mach = 0.34. In Fig. 9 right, the Delta PWL spectra provided by the design 1 at APP OP issued from all available methods are compared to each other. The WH and CAA solutions are fitting well the empirical "log law", whereas the acoustic performances assessed by LBM are weaker (in particular for the direct acoustic calculation). However, a PWL reduction of 3-5 dB (between 2kHz and 6 kHz) is expected from the LBM for both designs ON1 & ON2 as shown here after.

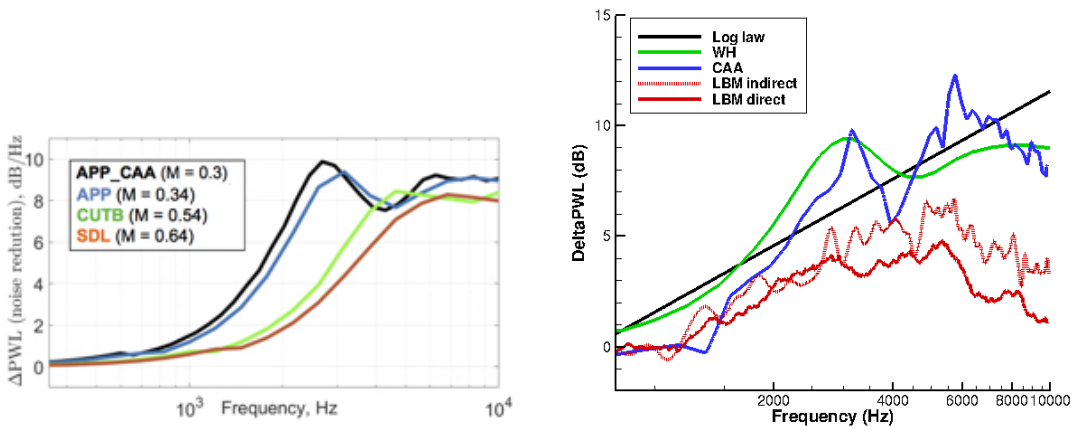


Figure 9 – Delta PWL spectra for design 1: WH solutions at 3 certification OP (left) and assessed from all different methods at APP (right).

5. Comparisons between predictions and first experimental results

5.1 Basic flow analyzes

The interaction noise radiated from the cascade airfoils is directly related to the upstream turbulent flow generated by the turbulence grid. Thus, a reliable capture of main characteristics is required to check the pre-test conditions used for the design and assessed from calculations. The single component turbulent velocity spectra, $S_{uu}(f)$, obtained from a single wire hot-wire probe at the location circled in blue in Fig. 3 are presented in Fig. 10 for two incident flow velocities, U_0= 45 m/s and 95 m/s (the higher reachable speed for a reliable use of the hot-wire data without vibration issues). They are compared to the standard Liepmann isotropic model (in blue) calibrated by experimental values for TI (turbulence intensity) and TLS (noted Λ), deduced from usual theoretical expressions (Eqs. (2-4) given below):

$$TI = \sqrt{\overline{u'^2}/U_0^2} \tag{2}$$

$$\overline{u'^2} = \int_{-\infty}^{+\infty} S_{uu}(f)\, df \tag{3}$$

$$\Lambda = \frac{U_0 S_{uu}(f=0)}{2\overline{u'^2}} \tag{4}$$

Practically, *u'* is restricted to the streamwise fluctuating velocity component. A solution based on a least square fitting method is plotted in red too. The values of TI and Λ are also provided in Table 3. Note that for $U_0 = 95$ m/s, the experimental spectrum was only used up to 10 kHz to estimate $\overline{u'^2}$ and Λ because of vibration issues. Overall, the Liepmann model provides a very good fit to the experimental data, with a decay slope in better agreement than the Von Karman model (not shown). The values of TI and Λ deduced from the theoretical expressions and from the least square fits are consistent with one another, and there seems to be some variations in these values between the two incident flow velocities considered. In Figure 11, the axial profiles of TI and TLS obtained from the LBM calculation are plotted from the grid plane region up to the cascade plane. As more detailed in the companion paper [10], the TLS from LBM is assessed by using the frozen turbulence approximation of Eq. (4), or applying the more rigorous definition based on the spatial correlation of streamwise velocity fluctuation. The values issued from the InnoSTAT experiment are plotted with dark symbols showing noticeable deviations with the numerical predictions for TI (around 5% from measurements instead of 3% from LBM) and TLS (around 12 mm from measurements instead of 9 mm from LBM). Note that previous data from Bampanis et al [4] related to comparable tests with slightly different set-up show a much better agreement with the present numerical predictions. Investigations are underway to try to explain these differences.

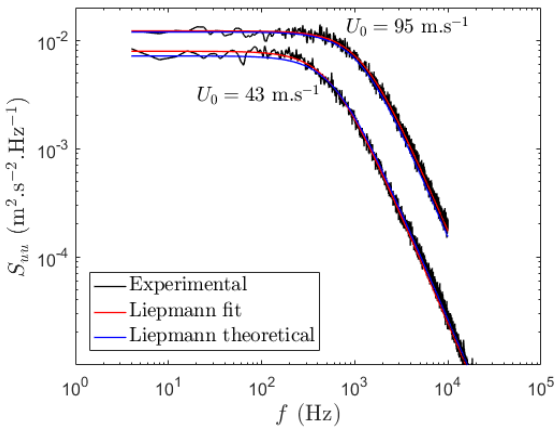


Figure 10 – Axial velocity spectra (Log scales) measured by HW and from Liepmann model.

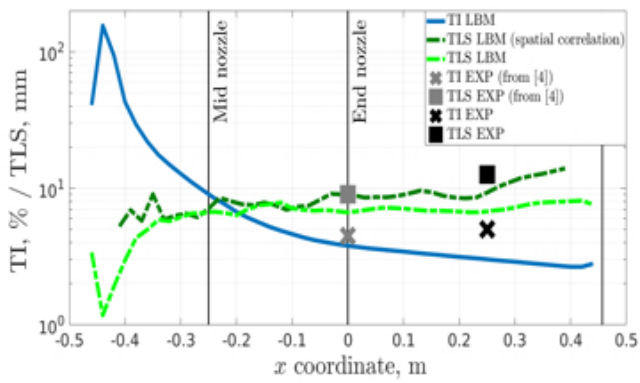


Figure 11 – TI and TLS profiles from LBM and local values from HW measurements.

Table 3 – Values of TI and TLS deduced from the experimental velocity spectra.

	$U_0 = 43$ m/s		$U_0 = 95$ m/s	
	TI (%)	Λ (mm)	TI (%)	Λ (mm)
Theoretical expression	6.1	11.2	4.9	13.3
Liepmann least square fit	6.5	11.2	5.0	12.6
Von Karman least square fit	6.5	11.2	5.4	11.4

Another essential aerodynamic behavior to be verified is the wall pressure coefficient (Cp). It is assessed on the reference vane at mid-span, for a flow speed of 117 m/s, and compared to RANS and LBM predictions in Fig. 12. A fairly nice agreement is pointed out between the three solutions.

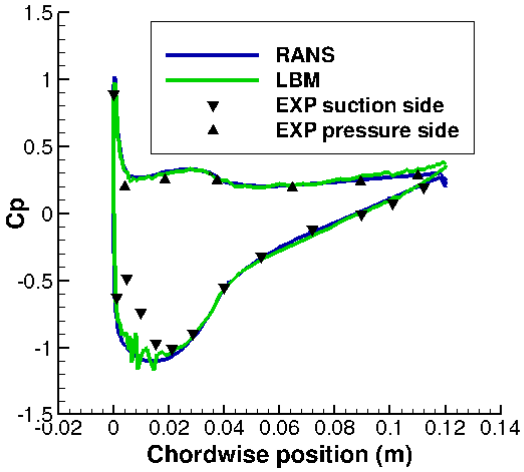


Figure 12 – Wall pressure coefficient from RANS, LBM and HW measurements.

5.2 Farfield spectra and OASPL directivities

This paragraph is devoted to the comparisons of SPL spectra at selected microphones of the farfield antenna and to OASPL directivities. The PSD measured at mic. 33 for the baseline and ON1 cases are plotted in Fig. 13, for all speed flow of the test matrix, from U_0 = 45 m/s (bottom curve) up to U_0 = 182 m/s (top curve). As expected, as long as U_0 is increased, the SPL are increased and the peak levels are shifted to higher frequencies. A significant level reduction can be observed for all speeds, and the cut-on frequency of treatment efficiency roughly varies linearly with U_0 (according to the Strouhal number $St=fh_s/U_0$).

Numerical predictions provided by CAA and LBM are compared to experiment in Fig. 14 left and right, for mics. 33 and 40, respectively. The agreement is good, in particular for the direct LBM solution, despite of the numerical dissipation effects of the mesh beyond 6.5 kHz (see [10]). Sawtooth variations sometimes visible on the experimental spectra (Fig 14, right) and fairly well captured by CAA and LBM too, can be attributed to cascade effects as discussed in [7].

OASPL directivity patterns are shown in Fig. 15, showing again a quite good matching between numerical predictions and measurements, despite an asymmetry effect with increased levels in the left arc [-90,-20°] compared to the right arc [40°,90°] more prominent in the experiments.

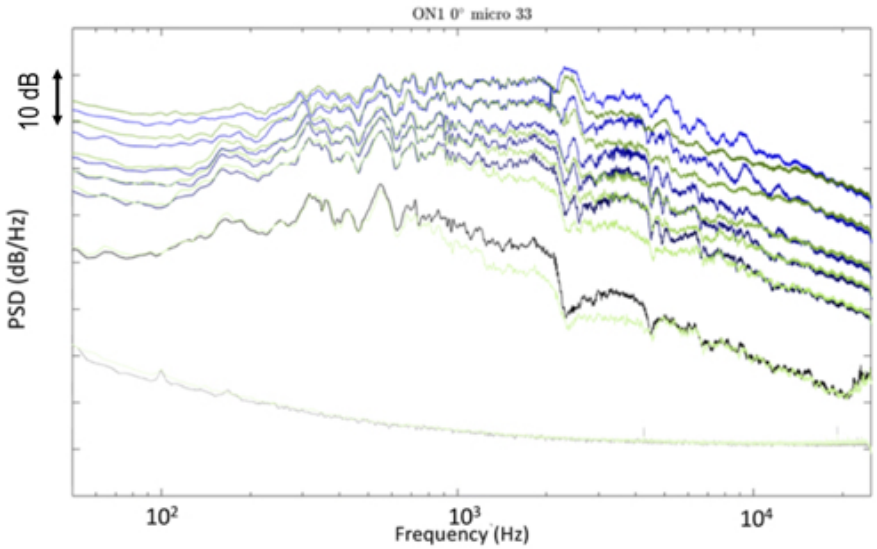


Figure 13 – Measured PSD at mic. 33 for baseline (in dark-blue) and design ON1 (in green) (6 flow speeds from 45 m/s to 182 m/s, the foot spectrum is the background noise without flow).

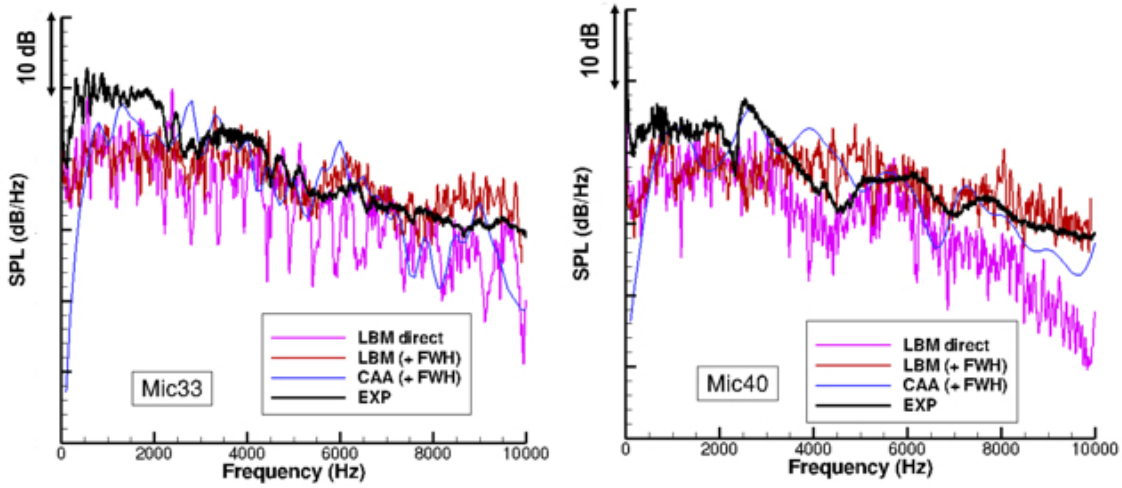


Figure 14 — PSD comparisons on baseline case: numerical simulations vs. experiment at Mach 0.34 for mic. 33 (left) and mic. 40 (right).

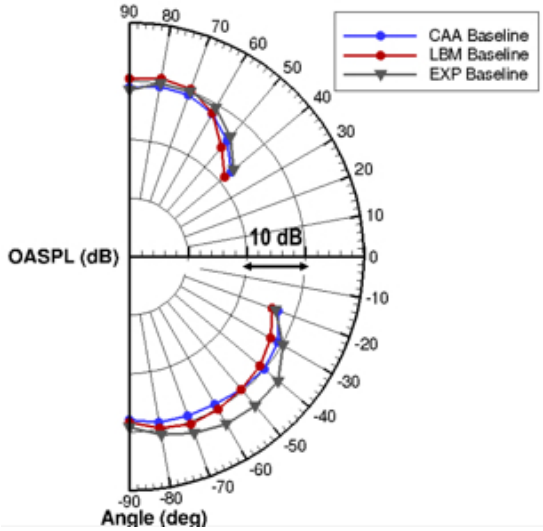


Figure 15 — Comparisons of OASPL directivities on baseline case (Mach 0.34).

5.3 Sound power level balance

The last acoustic analyzes are focused on the sound power spectrum (PWL) balance in order to assess the acoustic performances in terms of PWL reduction (DeltaPWL). To this aim, a simplified expression for sound power spectrum (W(f)) estimation proposed in [2,3,8] is adopted here too:

$$W(f) = \int_{-\pi/2}^{\pi/2} \frac{L_v R_{mic}}{\rho_0 c_0} |p_{mic}(f)|^2 d\theta \ , \ W_{ref}(dB) = 1E\text{-}12 \qquad (5)$$

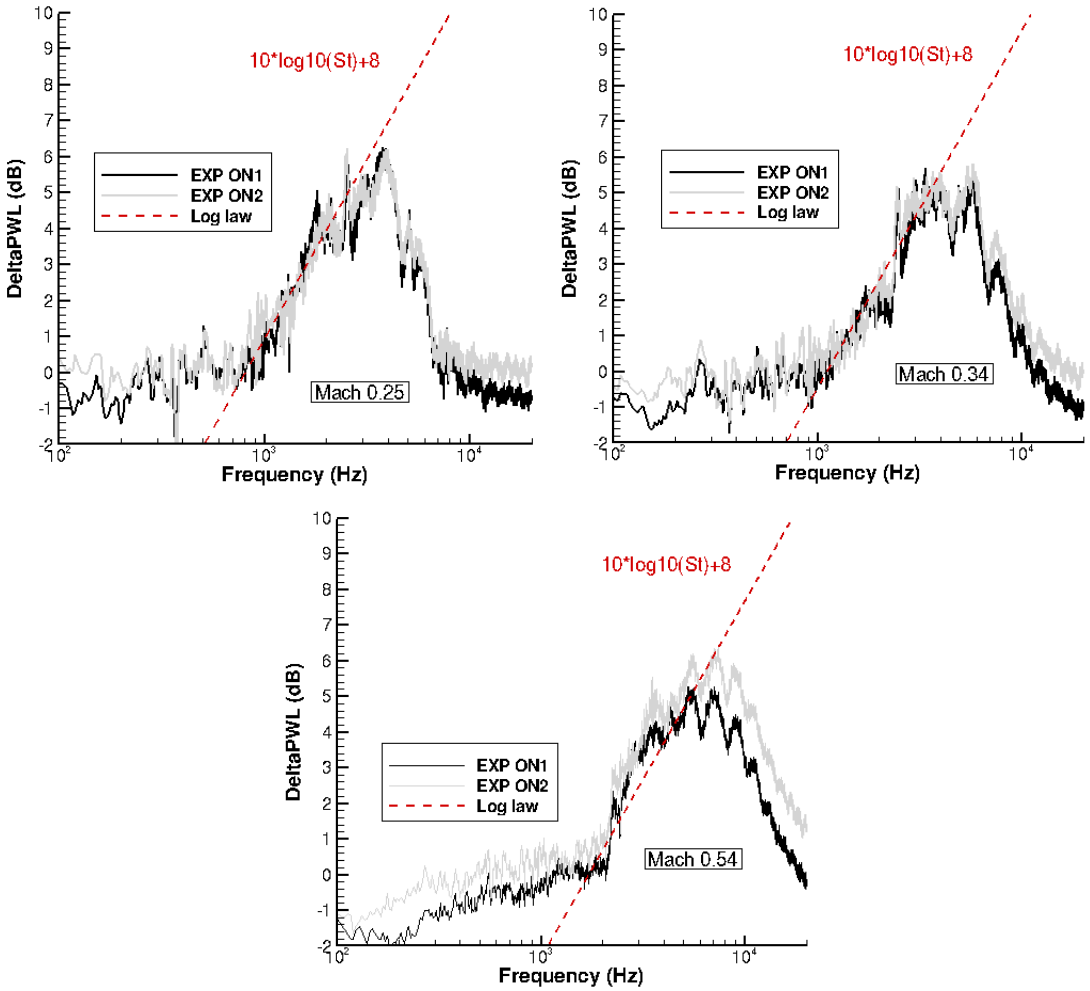


Figure 16 — DeltaPWL measured for ON1 and ON2 designs at 3 regimes: Mach 0.25 (left top), Mach 0.34 (right top), Mach 0.54 (bottom).

The DeltaPWL spectra so obtained from the measurements are plotted in Fig. 16 for the two designs (ON1 and ON2) and three flow regimes (Mach 0.25, 0.34, 0.54). A significant level reduction up to 6 dB can be observed with a peak frequency linked to the speed flow. Moreover, acoustic performances are found to be close with a slightly higher reduction for ON2, particularly at higher speed (Mach = 0.54). The "log law" is found to fit very well the experiment when the constant value in Eq. (1) is tuned from 10 to 8 dB. Note that tuning corrections of the original "log law" have been also suggested by Biedermann at al. [11] for an isolated airfoil experimental set-up.

DeltaPWL spectra provided by all available methods on design ON1 at Mach 0.34 (Mach 0.3 for CAA) are compared to the experiment in Fig. 17 (using a linear frequency scale contrary to Fig. 9). The WH and CAA solutions are close together but are displaying an overprediction of the PWL reduction. The LBM predictions are fairly well matching the measurements, and more particularly the direct LBM solution.

Finally, in Fig. 18 the DeltaPWL spectra provided by the direct LBM calculations at Mach 0.34 for designs ON1 and ON2 are successfully compared to the experiment, confirming the almost identical acoustic performances of both designs at this regime, and the high fidelity of the LBM approach.

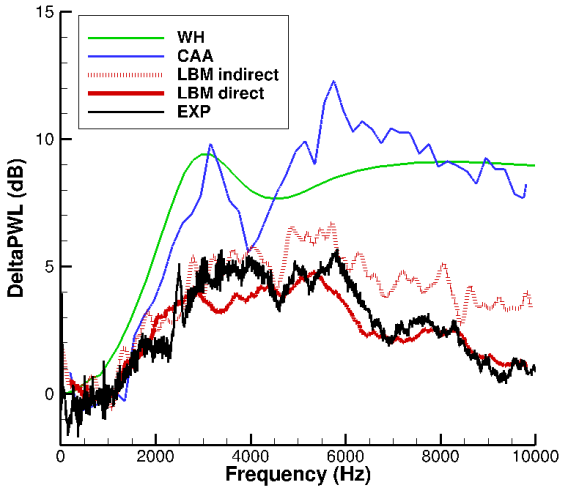


Figure 17 — DeltaPWL achieved by all methods for ON1 design and compared to experiment (Mach 0.34).

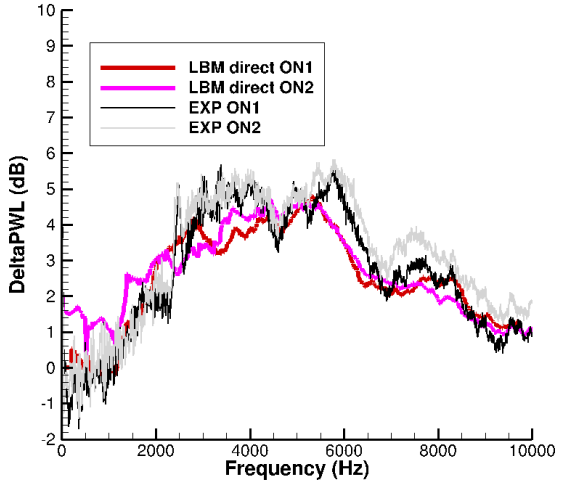


Figure 18 — DeltaPWL (dB) for ON1 & ON2 designs at Mach 0.34: direct LBM vs. experiment.

6. Conclusions

A comprehensive and complete work related to the aeroacoustic performances of a low-noise rectilinear cascade with LE serrations have been presented here. These investigations are a first step devoted to a laboratory experiment in which the inflow turbulence is generated by a grid (instead of fan blades) and the stator is approximated by a rectilinear cascade. Such a simplified configuration is essential to check the efficiency of selected passive treatments and to validate the prediction methods with respect to the turbulence-airfoil mechanism. The study has addressed both analytical/numerical and experimental activities with successful comparisons, adding a valuable scientific contribution regarding to the previous papers from the literature. After a brief overview of the design process and predicting methods (already presented) the focus has been set on the experimental set-up and instrumentation, and then to the comparisons between predictions and recently post-processed measurements. Two serrated low-noise cascade designs (denoted ON1 & ON2 here) proposed by Onera and selected by the Consortium of the InnoSTAT project have confirmed significant sound power level reductions (up to 6 dB) at different flow regimes with low penalties on aerodynamic performances (in particular for the ON2 geometry with an increased mean chord designed to this aim). The following highlights can be listed:

- Sinusoidal LE serrations applied to a rectilinear cascade (simplified OGV configuration) are definitively an efficient passive treatment able to produce sound power level reduction (4-6 dB) in a relevant frequency range (the frequency of maximum efficiency increasing with the speed flow);

- The acoustic predictions issued from Wiener-Hopf formulation (fast method) and CAA (mid-fidelity approach) are found to give reasonable trends but tend to overpredict the PWL reductions;
- The LBM simulations (detailed in a complementary paper) are believed to capture the main flow features (in terms of turbulent flow characteristics and wall pressure coefficient) involved in the turbulence-airfoil sound generation despite underpredicted values for TI and TLS (compared to hot-wire measurements recently post-processed).
- The DeltaPWL spectra (from designs ON1 & ON2) provided by the direct LBM solutions are in a fairly good agreement with the measurements, with similar acoustic performances obtained for the aerodynamically improved design ON2;
- The empirical "log law" from the literature is confirmed to give a reliable trend too, when the constants are tuned to better fit the present experimental conditions (as here, " PWL (dB) = 10log (St) + 8);
- Although not discussed in the paper, the flow incidence has a small impact on sound radiation and acoustic performances (regarding to the present measurements obtained with ± 8° deviations on nominal AoA).

Next step will be to extend this work to a realistic turbofan model with optimized serrated OGVs, adapted to turbulent blade wake charateristics including spanwise variations, as discussed in Ref. [5]. This is planned in InnoSTAT project, with another test campaign to be performed in the ECL-B3 facility at École Centrale de Lyon.

7. Contact Author Email Address

Please feel free to contact the main author at cyril.polacsek@onera.fr for further information.

8. Copyright Statement

The authors confirm that they, and/or their company or organization, hold copyright on all of the original material included in this paper. The authors also confirm that they have obtained permission, from the copyright holder of any third party material included in this paper, to publish it as part of their paper. The authors confirm that they give permission, or have obtained permission from the copyright holder of this paper, for the publication and distribution of this paper as part of the ICAS proceedings or as individual off-prints from the proceedings.

9. Acknowledgements

The authors would like to thank Safran Aircraft Engines for contributing to the technical requirements of the experimental test campaign. This collaborative work between ECL and ONERA has received respective funding from the Clean Sky 2 Joint Undertaking (JU) under the European Union’s Horizon 2020 research and innovation program under grant agreement n°865007 (InnoSTAT project), and from European Union’s Horizon 2020 research and innovation program in the frame of ADEC project of CS2 LPA-IADP. This publication reflects only the author's view and the JU is not responsible for any use that may be of the information it contains.

References

[1] Clair, V., Polacsek, C., Le Garrec, T., Reboul, G., Gruber, M. and Joseph, P., *Experimental and Numerical Investigation of Turbulence-Airfoil Noise Reduction Using Wavy Edges*, AIAA Journal, Vol. 51, No. 11, 2013.

[2] Narayanan, S., Chaitanya, P., Haeri, S., Joseph, P., Kim, J. W., and Polacsek, C., Airfoil Noise Reductions Through Leading Edge Serrations, Physics of Fluids, Vol. 27, No. 2, 2015.

[3] Paruchuri, C., Joseph, P., Narayanan, S., Vanderwel, C., Turner, J., Kim, J. W., and Ganapathisubramani, B., "Performance and mechanism of sinusoidal leading edge serrations for the reduction of turbulence–aerofoil interaction noise," Journal of Fluid Mechanics, Vol. 818, 2017.

[4] Bampanis, G., Roger, M., Ragni, D., Avallone, F., Teuna, C, *Airfoil-Turbulence Interaction Noise Source Identification and its Reduction by Means of Leading Edge Serrations*, *25th AIAA/CEAS Aeroacoustics Conference*, Delft, The Netherlands, May 20-23, 2019.

[5] Polacsek, C., Cader, A., Buszyk, M., Barrier, R., Gea-Aguilera, F., and Posson, H., *Aeroacoustic Design and Broadband Noise Predictions of a Fan Stage with Serrated Outlet Guide Vanes*, Physics of fluids, Vol. 32, No. 10, 2020, p. 107107.

[6] Finez, A., *Etude expérimentale du bruit de bord de fuite à large bande d'une grille d'aubes linéaire et de sa réduction par dispositifs passifs*, Ph.D. thesis, Ecole centrale de Lyon, France, 2012.

[7] Buszyk, M, Polacsek, C., Le Garrec, T., Barrier R., Bailly, C., *Numerical Assessment of Turbulence-Cascade Noise Reduction and Aerodynamic Penalties from Serrations*, AIAA Journal (published online 17 March 2022), https://doi.org/10.2514/1.J061301.

[8] Buszyk, M, Le Garrec, T., Polacsek, C., Barrier, R., *Lattice Boltzmann simulations in a rectilinear cascade configuration for the turbulence-airfoil interaction noise evaluation and reduction through serrated leading edges*, Euronoise 2021 (online conference), Madeira (Portugal), 2021.

[9] Ayton, L., and Paruchuri, C., "An analytical and experimental investigation of aerofoil–turbulence interaction noise for plates with spanwise-varying leading edges," Journal of Fluid Mechanics, Vol. 865, 2019, pp. 137–168.

[10] Buszyk, M., Vienne, L., Le Garrec, T., Boussuge, J. F., Polacsek, C., and Barrier, R., *Numerical benchmarking of LBM simulations applied to turbulence-cascade configurations*, ICAS 2022, September 4-9, 2022.

[11] Biedermann, T. M, Czeckay, P., Geyer, T. F., Kameier, F., Paschereit, C. O., *Effect of Inflow Conditions on the Noise Reduction Through Leading Edge Serrations*, Technical Notes, AIAA Journal, Vol. 57, No. 9, 2019, https://doi.org/10.2514/1.J057831.